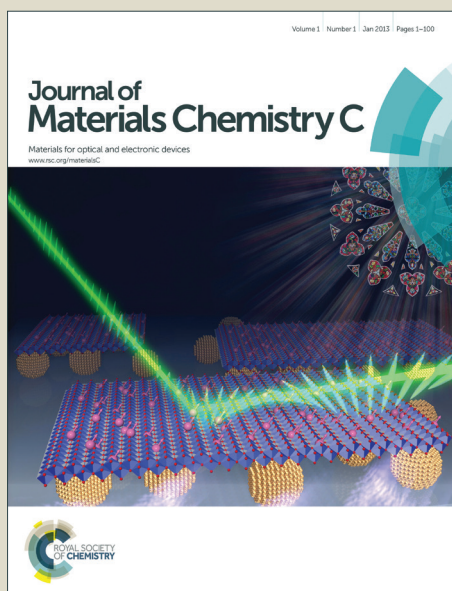


Journal of Materials Chemistry C

Accepted Manuscript



This is an *Accepted Manuscript*, which has been through the Royal Society of Chemistry peer review process and has been accepted for publication.

Accepted Manuscripts are published online shortly after acceptance, before technical editing, formatting and proof reading. Using this free service, authors can make their results available to the community, in citable form, before we publish the edited article. We will replace this *Accepted Manuscript* with the edited and formatted *Advance Article* as soon as it is available.

You can find more information about *Accepted Manuscripts* in the [Information for Authors](#).

Please note that technical editing may introduce minor changes to the text and/or graphics, which may alter content. The journal's standard [Terms & Conditions](#) and the [Ethical guidelines](#) still apply. In no event shall the Royal Society of Chemistry be held responsible for any errors or omissions in this *Accepted Manuscript* or any consequences arising from the use of any information it contains.

Effect of head group size on the photoswitching applications of azobenzene disperse-red 1 analogues

Cite this: DOI: 10.1039/x0xx00000x

Alexis Goulet-Hanssens,^{a,b} T. Christopher Corkery,^a Arri Priimagi,^c Christopher J. Barrett^a

Received 00th January 2012,
Accepted 00th January 2012

DOI: 10.1039/x0xx00000x

www.rsc.org/

We investigate the effect of increased molecular bulk in the 'head' group for a class of newly synthesized azobenzene class chromophores with a clickable ethynyl group *para*, and a nitro group *ortho* to the azo bond on the distal benzene ring. This 'variable-head' functionalization provides a family of dyes with photophysical character very similar to Disperse Red 1, one of the most commonly used azo dyes in materials science. Phenyl, naphthyl, and anthracyl derivatives were synthesized as small molecules, monomers, homopolymers, and copolymers in a rapid and facile manner using click chemistry, confirming the versatility of this parent chromophore. Photochemical and spectral studies indicate that this strategy is suitable to build a 'bulkiness series' of stimuli-responsive materials, as the various material derivatives retain the absorption and kinetic character of the parent chromophore necessary for all-optical patterning applications that DR1 dyes have been optimized for. In thin films, larger head group size was found to increase the stability of light-induced birefringence in copolymers. The homopolymers formed stable surface-relief gratings upon interference irradiation, whose grating depths correlate with head group size, demonstrating that this new class of polymers can also undergo tailored macroscopic photoinduced motions, which could have applications in all optical nano-patterning.

Introduction

Light-responsive applications requiring reversible, easy and rapid actuation is critical to the materials' success often rely on azobenzene as the working photoswitch. The light-triggered isomerization of the azobenzene (azo) chromophore from the *trans*- to the *cis*- geometries when irradiated with visible light drives material response, and Disperse Red 1 (DR1) -based azo materials can impart large changes to surface properties and macromolecular structures.^{1,2} Overlapping *cis*- and *trans*-absorption bands make this class of chromophore well suited for All Optical Nano-Patterning (AONP) such as surface relief gratings (SRG) formation, photoinduced birefringence studies and photomechanics³⁻⁵ since many reconversion cycles can be triggered by the same wavelength of light. This is possible due to the push-pull feature of the amino and nitro substituted groups across the azo bond in DR1 (1, Figure 1) which provides a red-shifted absorbance far into the visible as well as a far faster thermal reconversion of the *cis*- to the *trans*-state.⁶ These AONP light-driven phenomena are now best-thought to be caused by free volume changes of the azobenzene as it

undergoes its *trans-cis-trans* isomerization cycle,⁷⁻⁹ which motivates our current study.

The ability to increase or tune the degree of free-volume change during isomerization would allow for improved design of current materials. To explore this optimization we designed and prepared analogues (**Figure 1**) that maintain the features that make DR1 the main azo-workhorse in materials literature, while providing an easily functionalizable 'head' group. The pseudo-stilbene chromophore, **2**, features a 4-4' push-pull amino-nitro structure across the azo bond that makes its absorption well suited for rapid reversible actuation by lamp or laser irradiation. Relocating the nitro group from the *para* position to an *ortho* position retains the push-pull across the azo

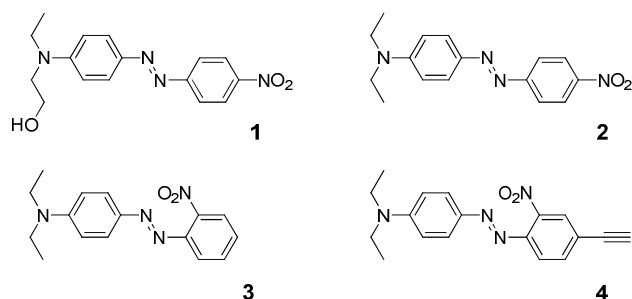


Figure 1. The chromophores DR1 (1), diethylaniline-DR1 (2), *ortho*-DR1 (3), and ethynyl *ortho*-DR1 (4).

bond while freeing the *para* position, considered to be the most important in terms of effecting photoinduced changes in free volume,^{10,11} for further functionalization. Although the *ortho* structure (3) has been known for decades, it has only been studied in depth in the commercial dye literature,^{12,13} and not in the context of functional materials. Placing an ethynyl group in the *para* position (4) allows for rapid functionalization using now-common copper-catalyzed alkyne azide cycloaddition (CuAAC, or ‘click’) chemistry.¹⁴ As we report in a previous publication, this approach is an easy and versatile way to rapidly generate diverse azo structures while maintaining the switching properties of the unfunctionalized dye.¹⁵

A possible reason these *o*-nitro structures have been absent in the materials literature can be attributed to evidence that functionalization of azo dyes *ortho* to azo bond can decrease their photostability.^{16–18} In investigating this issue, photostability has been studied for several diethylaniline dyes including DR1 (1) and its *ortho* analogue (3). It was reported that both of these dyes photodecompose, with *ortho*-DR1 bleaching faster than DR1 in acetone solutions in the presence of oxygen, however, in deoxygenated acetone solutions or crystalline forms the *ortho* species is more stable than DR1.¹⁹ Given the impact DR1 has had in the literature, with proper engineering and selection of handling parameters, *ortho*-DR1 could also act as a viable tool in materials science.

To determine the effect of the head group on the dye properties, structure 4 was reacted with aryl azides to form new ‘head’ groups bearing increasingly larger functionality (Figure 2). These were used to investigate the effect free volume changes had on the photoisomerization of these structures. To help elucidate the results observed in these materials, small molecule analogues, monomers, and homopolymers of the three derivatized azos were synthesized. As a proof of concept of the variable preparation of these structures, copolymers were prepared by diazotization as a mechanism of macromolecular post-functionalization²⁰ which could then be ‘clicked’ to the final chromophore structure. All of these structures can be easily attained using click chemistry, providing derivatives with similar optical properties.

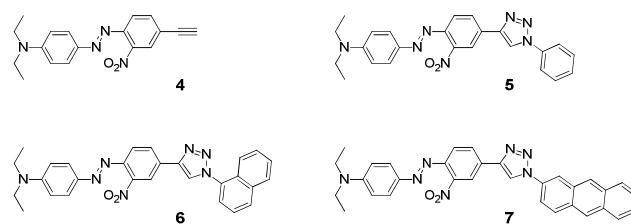


Figure 2. Structures of the four model dyes (4–7) used in this study.

Experimental

Material Syntheses

With the goal of keeping these syntheses as facile as possible, using the mildest conditions allowable, all reactions except for Sonogashira couplings and polymerizations (dry solvent, nitrogen atmosphere) were conducted under atmospheric conditions at room temperature. ¹H NMR spectra were acquired at 298 K, on a Varian-Mercury 300 MHz or 400 MHz spectrometer while ¹³C NMR spectra were acquired on a Varian-Mercury 300 MHz NMR spectrometer. Chemical shifts are reported in ppm on the δ -scale referenced to either the solvent signal or internal TMS standard. High resolution mass spectrometry (HR-MS) was acquired on a Thermo Scientific Exactive Plus Orbitrap. Samples were ionized using either atmospheric-pressure chemical ionization (APCI) or electrospray ionization (ESI). All observed ions in positive and negative ionization modes are reported. All chemicals were obtained from Sigma-Aldrich corporation (St. Louis, MO, USA), with the exception of trimethylsilylacetylene which was obtained from Oakwood Chemicals (West Columbia, SC, USA). For synthetic details, please see the electronic supplementary information file.

Polymer Synthetic Approach

Homopolymer samples were prepared by free-radical polymerization of pure monomers in THF initiated thermally by AIBN. For the copolymer an approach to functionalize a common batch of azo precursor polymer through a diazotization reaction with an ethynyl-bearing head group (akin to 4) which could then be ‘clicked’ for further functionalization was targeted. To maintain high solubility of the azo side chains a target functionalization of 2 mol-% was attempted. Absolute characterization of the monomer dye content was impossible within a reasonable margin of error using NMR. The absorption coefficient of the copolymer dyes is expressed as a mass extinction coefficient (ESI), and the dye content for all copolymers was found to be between 0.8 and 2.1 mol%. Homopolymers were found to have molecular weights ranging between 2,490–3,560 g/mol while the copolymers had molecular weights ranging 9,350–10,390 g/mol. Low azo content is critical for optimal processing abilities in these higher molecular weight polymers, and this low dye content allows for efficient photoisomerization in the solid state and the inscription of photoinduced birefringence.^{21,22} Further details can be found in the Electronic Supplementary Information.

Optical Characterization in Solution

Solution characterization of the small molecules and polymers was conducted in dry spectral grade THF on a Cary Bio 300 UV/vis spectrophotometer to measure the absorption spectra and λ_{max} values. The isomerization kinetics were measured with a Melles Griot Series 43 Ar⁺-ion laser with emission at 488 nm that was set up in a pump-probe arrangement, as shown in **Figure S15**. Thermal decay of the *cis*- to *trans*-state was monitored by examining the transmittance of the samples over time: upon pump cycle, the absorbance of the sample solutions at 488 nm (which is used for both pumping and probing) decreases due to *trans*-to-*cis* isomerization, and the thermal *cis*-*trans* reconversion shows up as an intensity decrease (absorbance increase) over time. The power of the pump beam was ~ 300 mW/cm² with a pump cycle of between 5 and 10 seconds to induce isomerization and ensure sample saturation back to the *trans* state. The probe beam was chopped mechanically at 1410 Hz, attenuated, and passed through the sample into a photodiode detector, where the intensity was recorded as a function of time. The pump irradiation time (~ 100 – 200 ms) was short enough to avoid heating the sample, so the kinetic measurements can be considered to have been acquired at room temperature.²³

Optical Characterization of Thin Films

The photoresponsive properties of the homopolymers and copolymers were also studied as thin films. The polymers were dissolved in THF and spin coated onto clean glass substrates to yield films with thicknesses in the range of 500 nm (homopolymers) and 1.5 μm (copolymers). A thin film (150 nm) of the commercially available poly(DR1 acrylate) (Sigma-Aldrich) was used as a reference. All films were homogeneous and isotropic as verified with polarized optical microscopy. The films were characterized with photoinduced spectral changes, birefringence, and surface-relief grating formation, using a collimated and spatially filtered 488 nm Ar⁺-ion laser as a pump. The excitation was carried out either with circularly polarized (photoinduced spectral changes, 50 mW/cm²) or horizontally polarized (photoinduced birefringence, 150 mW/cm²; SRG formation, 300 mW/cm²) light beam.

The absorption spectra in the dark and during irradiation (488 nm, 50 mW/cm²) were measured with a fiber-optic spectrometer (Ocean Optics USB2000+) using a deuterium tungsten halogen lamp as a light source (Ocean Optics DH-2000-BAL). The photoinduced birefringence was measured with a normally incident probe beam from a diode laser ($\lambda = 820$ nm). The transmitted intensity of the probe beam through a polarizer/sample/analyzer combination was monitored with a photodiode. The orientation of the polarizer/analyzer was set to $\pm 45^\circ$ with respect to the polarization of the excitation beam, and the birefringence $|\Delta n|$ was calculated from the transmission data I as $|\Delta n| = \lambda(\pi d)^{-1} (I/I_0)^{1/2}$, where I_0 is the photodiode signal for a parallel polarizer/analyzer orientation (in the absence of the sample) and d is the film thickness. The SRGs were inscribed in a Lloyd mirror configuration by directing half of

the expanded incident beam directly onto the sample and reflecting the other half from a mirror set at right angle with the sample. The period of the resulting interference pattern was set to *ca.* 1 μm . The build-up of SRGs was monitored in real time by measuring diffraction from a $\lambda = 820$ nm probe beam. The height profiles of the inscribed SRGs were determined by atomic force microscopy (Veeco Dimension 5000 SPM).

Results and Discussion

Comparing *o*-DR1 to DR1

The absorption spectra and extinction coefficients for **2** and **3** are detailed in the ESI (**Figure S1**). The *ortho*-nitro species absorbance is blue-shifted, with a λ_{max} of 452 nm, as opposed to the 489 nm λ_{max} in **2**. This 37 nm shift in the absorption maximum is on the order of generally observed shifts seen in polyenes upon addition of an extra π system, and may be due to a shorter Hückel conjugation length in the donor-acceptor ends of the azobenzene.^{24,25} In terms of their thermal *cis*-*trans* isomerization, the *ortho*-DR1 species relaxes significantly faster than the native DR1 dye in solution, with a half-life of 0.13 seconds compared to 1.1 seconds. This order of magnitude increase in speed is possibly due in part to a more sterically hindered *cis* state due to the *ortho*-nitro group, which would accelerate reconversion.²⁶ Overall, with the change to the *ortho* species, the desirable absorbance is retained and the rapid reconversion is improved. This latter fact permits more switching cycles per unit time, increasing the effective work done by photoresponsive materials as more time is spent in the active switching portion of the isomerization cycle. In all of our solution-based optical studies we have observed successful switching for 100's of cycles without a decrease in switching behaviour.

Molecular Dyes

Model Compounds with different *para*-substituents were prepared by functionalizing **4** using 'click' chemistry (**Figure 2**). As we sought to explore architectures that provided little or no electronic effect to the azo chromophore and varied solely in their molecular size, phenyl- (**5**), 2-naphthyl- (**6**), and 1-anthracyl- (**7**) functionalized dyes were prepared. In these dyes, the electron donation of the amine is balanced slightly with the l' amine of the triazole, resulting in a slight decrease in the push-pull effect from the nitro group to the diethyl aniline amine. This leads to a consistent hypsochromic shift in the absorbance wavelength with respect to the λ_{max} of the parent compound (**4**), as seen in **Figure 3**. Additionally some of the anthracene $\pi \rightarrow \pi^*$ transitions between 300 and 400 nm are clearly evident as fine features.²⁷

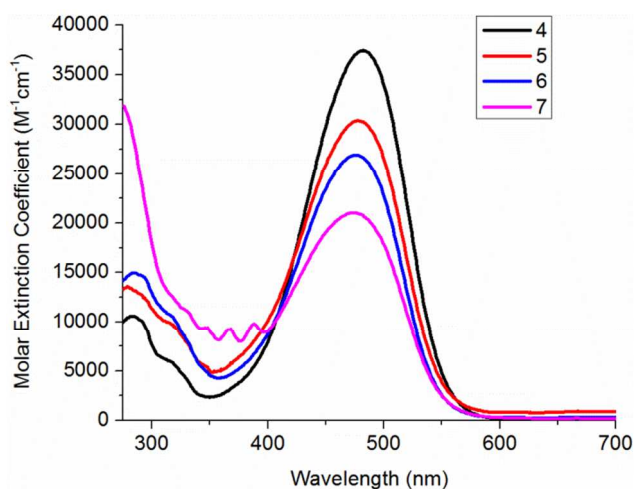


Figure 3. UV-vis spectra of 'clickable' (**4**) and 'clicked' (**5-7**) small molecules in THF.

The kinetic decays of the model dyes are first order (**Figure 4**) and the time constants are given in **Table 1**. The half-life increases systematically with increasing size of the head group, from 0.18 s for the native dye (**4**) to 0.74 s for the naphthyl (**6**) and anthracyl (**7**) derivatives. As the diethylamino "tail" is identical in all instances, this indicates that the larger molecular size of the head group leads to slower thermal relaxation. This finding suggests that the *para* functionalization should not cause prohibitive steric hinderance in the *cis* state, which would cause these dyes to perform poorly as switches.

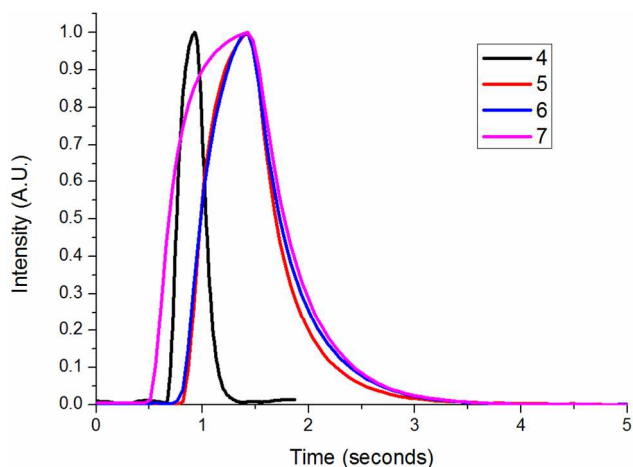


Figure 4. Absorbance normalized pump-probe cycles for small molecules **4-7** in THF, showing the increase in *cis* state upon irradiation and thermal reconversion to the stable *trans* state.

After validation of the approach using small molecules, model monomer compounds, shown in **Figure 5**, were studied as an intermediate step between the model dyes and polymers to elucidate the effect of further functionalization on the azobenzene tail to the photoresponse of these chromophores. As with the model compounds, the 'clicked' monomers (Compounds **9-11**) λ_{max} blue shift from the 'unclicked' form (Compound **8**), as seen in **Table 1**, and also show a similar

slowing of the thermal relaxation rate with increasing size of the clicked moiety, since the single bond character of the azo bond decreases with the competing intra-ring electron donation. The addition of the methacrylate tail causes a significant increase in the $t_{1/2}$ when compared to the non-monomer dyes. A possible explanation for this observation is that there is no longer one side that preferentially moves while the other remains still in the isomerization event. Similar to the decay rate being decreased with higher molecular head size, all of the monomers now show a slower thermal relaxation to the *trans* state than their corresponding non-monomer forms, since all possess a larger 'tail' group.

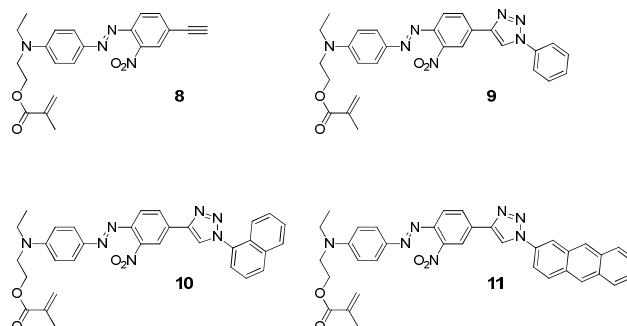


Figure 5. Structures of the four model monomer dyes (**8-11**) used in this study.

Table 1. λ_{max} , and $t_{1/2}$ for model diethyl-aniline Compounds **4-7** and monomer Compounds **8-11** in THF.

Compound	λ_{max} (nm)	$t_{1/2}$ (seconds)
2	489	1.10
3	452	0.13
4	482	0.18
5	477	0.57
6	476	0.74
7	473	0.74
8	471	0.36
9	465	1.45
10	467	1.61
11	468	0.93

Macromolecular Dyes

Homopolymers (Compounds **12-14**, **Figure 6**) were prepared by free radical polymerization of pure monomers (**9-11**), to verify the behaviour of these novel azos in pure polymeric form.

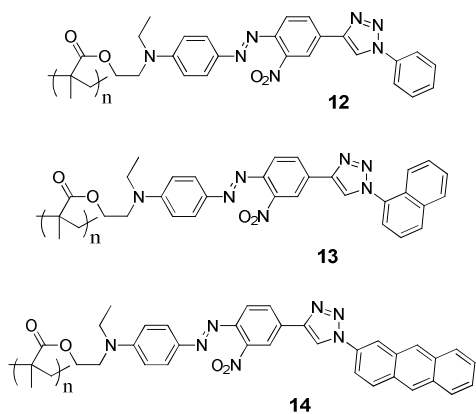


Figure 6. Structures of the phenyl, naphthyl and anthracyl homopolymers (**12–14**) used in this study.

The absorption profile (**Figure S9**) of the three homopolymers in solution remains the same as for the corresponding monomers, showing that polymerization has no effect on the absorption of the azo dyes. The decay kinetics (**Table 2**) of homopolymers **12–14** have similar trends to the small molecule dyes **5–7** in terms of half-lives. As the molecular size increases, the thermal reconversion slows down, due to a larger molecular ‘arm’ that has to be moved. However, overall we generally observe faster isomerization rates than in the monomer form. This is likely due to the more sterically congested *cis* states and suggests that molecular architecture has a large effect on determining the baseline isomerization rate, with the trend in ‘head’ size determining the relative rates.

Copolymers were synthesized by polymer post-functionalization as opposed to copolymerization (**Figure 7**). This was done as a proof of concept, since diazotization has grown in prominence as an easy way to generate amphiphilic photoresponsive polymers,²⁰ and could also be used to generate complex functional polymers. As mentioned above, azo copolymers synthesized from monomers can suffer from low molecular weights and high chromophore aggregation, two factors that are non-desirable in creating polymers for use in materials applications. The approach employed here²⁸ solves both of these issues as all diversified polymers have the same ~10,000 g/mol molecular weight and spaced chromophore placement.

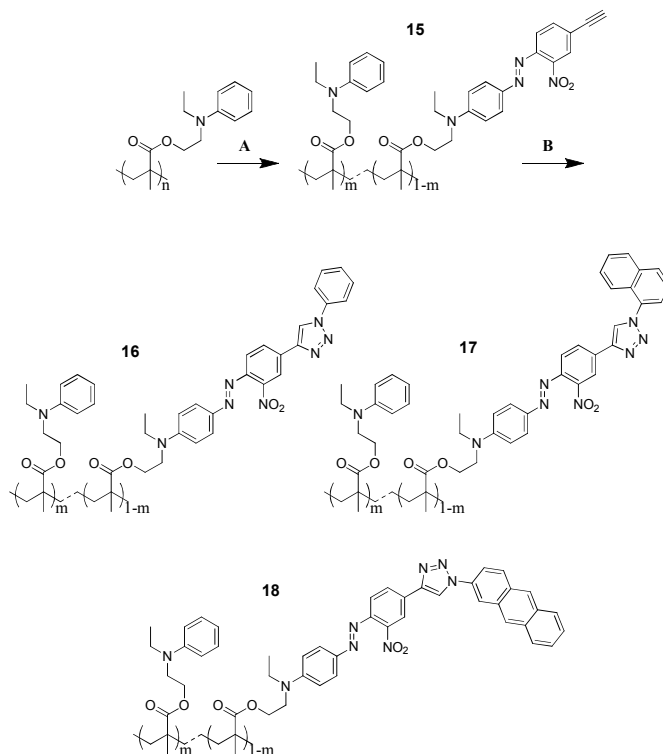


Figure 7. Strategy for achieving diversified azo copolymers. An N-ethyl anilino ethanol methacrylate homopolymer is diazotized in step A to form an azo copolymer (**15**). This copolymer can be diversified in step B with any head group to create a functionalized azo copolymer (**16–18**).

The spectra of the functionalized polymers (**Figure S11**) show a bathochromic shift in λ_{\max} to 473 nm, as compared with 464 nm in the starting material (**15**). These polymers exhibit thermal reconversion that is best fitted by a biexponential decay function. The fast component, as shown in **Table 2** increases in speed as the monomer head size increases. The observed data indicates similar behaviour to the monomer species, and most likely does not mimic the homopolymer model as there is less steric hindrance in these farther-spaced chromophores than in the homopolymer. As with the homopolymer series, the polymeric forms of the dyes are more sterically crowding leads to increased rates in the fast relaxation component, which is evidenced in all derivatives.

Table 2. λ_{\max} , $t_{1/2}$, and Mw for homopolymers **12–14** and for copolymers **15–18** in THF.

Compound	λ_{\max} (nm)	t_a (s)	t_b (s)
12	466	0.77	---
13	466	0.65	---
14	466	1.1	---
15	464	0.51	---
16	473	0.47	2.49
17	472	0.23	1.26
18	454*	0.34	1.53

*The absolute absorbance peak for the anthracyl derivative is an anthracene feature atop the azo feature, the azo feature itself is comparable to the other two derivatives at ~470 nm.

Thin Films

While solution data yields important information on the trends between different molecular structures, the photoresponsive behaviour within thin azo-polymer films is of greater practical interest. Spun-cast films were investigated first for their isomerization potential as the chromophores are in a much more tightly packed environment. Acquiring UV/vis spectra in thin films under constant irradiation allowed us to measure the photostationary state of the chromophores. The copolymer **15** can achieve a relatively large *cis*-population upon irradiation, as evidenced by the 15 % decrease in absorbance (Figure 8a). As the head group is increased in size in the copolymer family a notable drop in *cis*-content is measured (Table 3): the drops in absorbance are 11 %, 8 %, and 5 % for the phenyl, naphthyl, and anthracyl-functionalized copolymers, respectively. For the homopolymers **12** and **13** (high-quality films of **14** could not be formed) the light-induced decrease in absorbance is quite negligible, meaning that only a very small fraction of the molecules converts to the *cis* state. This indicates that in homopolymers, smaller co-monomers are critical to permitting a reasonably high *cis* state in the bulk material (Figure 8b).

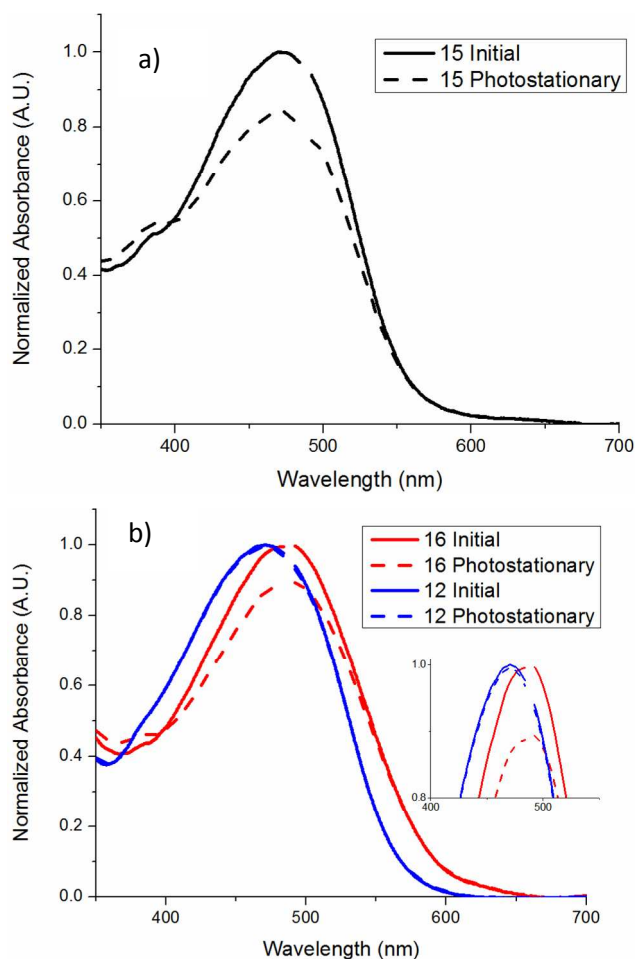


Figure 8. (a) Isomerization extent of a film of polymer **15** spun cast on a clean glass substrate from THF, demonstrating an absorbance decrease of 15% under constant irradiation, (b) The blue-shift and decrease in absorbance change when homopolymer **12** is compared to copolymer **16** under constant irradiation. Irradiation in both figures with a 488 nm Ar⁺ laser at 50 mW/cm² intensity.

Table 3. Absorbance decreases in the polymer films when excited at 488 nm.

Polymer	Isomerization Extend in Film	λ_{\max} (nm)
#12	0.5%	471
#13	1%	475
#15	15%	472
#16	11%	485
#17	8%	483
#18	5%	468

Figure 9 presents the photoinduced birefringence curves for the copolymers **15–18**. Due to the low azobenzene content, the absolute birefringence is relatively low for all samples, but comparable to copolymers²² and doped polymers²⁹ containing low concentration of DR1. For all samples, the birefringence can be erased with circularly polarized light and rewritten on the same spot without fatigue. Like the isomerization efficiency, the birefringence decreases systematically with increasing size of the head group, suggesting that it is more difficult for larger molecular moieties to move within the polymer matrix in response to irradiation with polarized light. The decreased mobility is further supported by the fact that the residual birefringence increases with the head group size, indicating that the free-volume change during isomerization drives a more stable reorganization of the polymer film. No SRGs could be inscribed into the copolymers, which can be attributed to the low content of the azobenzene moieties.

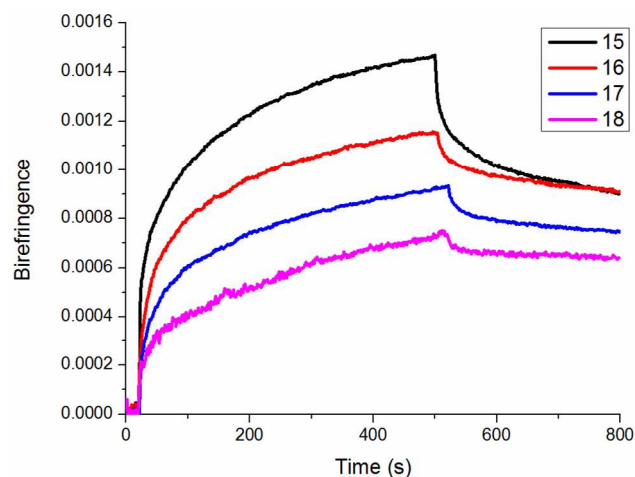


Figure 9. Photoinduced birefringence in copolymer samples **15–18**, demonstrating reduced birefringence with increased head group size. The writing beam is turned on at 30 s, and the irradiation is ceased at 500 s.

Even though homopolymers **12** and **13** exhibit very low isomerization efficiency, we successfully inscribed SRGs onto films of both polymers using interference irradiation. The build-up of the gratings was followed by monitoring the first-order diffraction in real time, as shown in Figure 10a. Contrary to the photoinduced birefringence, the SRG formation

efficiency is higher for the naphthyl-substituted dye (**13**) than for the smaller phenyl-substituted dye (**12**). Hence macroscopic molecular movements seem to be enhanced by employing a molecular switch requiring larger free-volume change upon photoisomerization. Yet we note that compared to the widely used and commercially available homopolymer poly(Disperse Red 1 acrylate), which can be used as a gold standard for SRG applications, the grating formation efficiency is low (**Figure 10a**).

Another explanation for the higher diffraction efficiency of **13** as compared to **12** may be lesser chromophore packing between neighbouring azobenzene units, due to the larger head size group size of **13** and the rotational symmetry of **12**. This is supported by the observation that when comparing the corresponding homo- and copolymers (**12** vs. **16**; **13** vs. **17**) the blue-shift in the absorption spectrum – indicative of chromophore-chromophore intermolecular interactions^{22,30} is more pronounced for the phenyl-containing systems (*ca.* 14 nm; see **Figure 10b) than for the naphthyl-containing systems (*ca.* 8 nm). The difference is small yet clearly evident, providing a plausible explanation for the lower isomerization efficiency of **12** with respect to **13**, converse to the copolymers, for which **16** displays larger decrease in absorbance upon irradiation than **17**.**

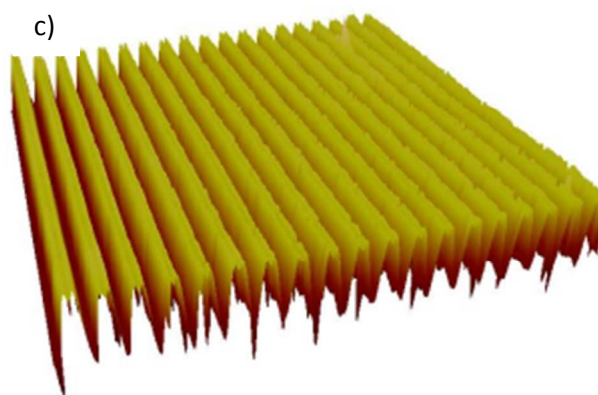
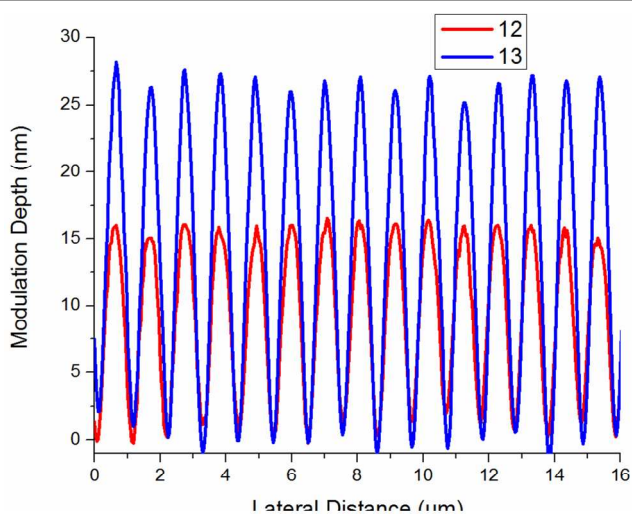
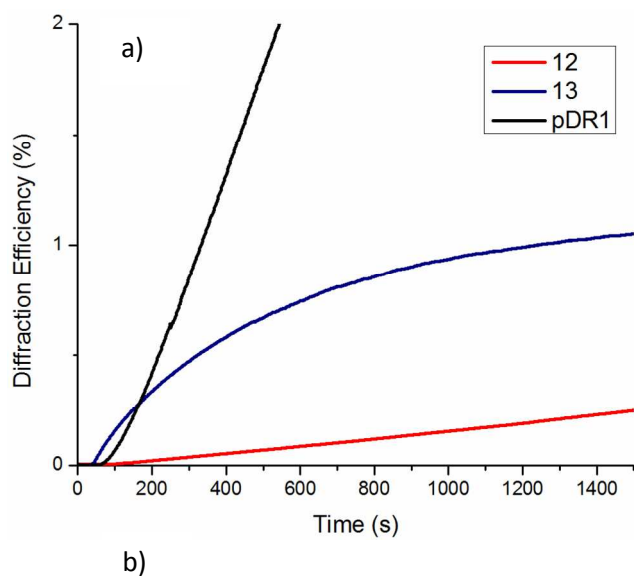


Figure 10. (a) First order diffraction efficiency as a function of irradiation time for pDR1A as a reference and homo-polymers **12** and **13**, (b) measured modulation depth in the films for polymers **12** and **13** (c) 3-D AFM plot of surface relief grating formed by 300 mW/cm² 488nm Ar⁺ laser light in a thin film of polymer **13**

The existence of stable SRGs on thin films of **12** and **13** was verified by imaging the sample surfaces with an atomic-force microscope. The surface-modulation depths, as shown in **Figure 10b**, are *ca.* 15 nm and 27 nm for **12** and **13**, respectively, and a 3D view of an SRG inscribed on **13** is shown in **Figure 10c**. The modulation depths are in line with the diffraction curves shown in **Figure 10a**, since at the small-modulation-depth regime the diffraction efficiency is expected to scale quadratically with the modulation depth.³¹ Even if the achieved modulation depths are modest given that depths of hundreds of nm can be obtained, we note that only a vanishingly small fraction of the azobenzene molecular motors participates in driving the macroscopic motions in these systems. Hence we believe that once the materials composition is properly optimized, the photoinduced motions driven by the azo moieties reported in this work can be greatly enhanced.

Conclusions

We synthesized and tested a variety of complex azo architectures based on a novel *ortho*-DR1 dye with a ‘clickable’ *para*-ethynyl group that retains actuation and relaxation

properties while allowing for rapid structural variation. This model was validated in small molecule, monomer, homopolymer as well as in post-functionalized copolymer schemes. With the exception of the copolymer species, the λ_{\max} of these chromophores shows a modest blue shift after 'click' functionalization. Post-functionalization accelerates the decay kinetics of the dyes in solution, a fact that may seem counter-intuitive if considering only molecular size and not steric hindrance in the *cis* state. Homopolymers of these structures exhibit only a 0.5–1% decrease in absorbance upon irradiation, demonstrating limited *cis* content, yet could form relatively large depth surface relief gratings. Copolymers made from a post-functionalization strategy exhibited stable photoinduced birefringence, with the long-term stability being determined by the 'head' group size.

Together these findings indicate that the free-volume change that azobenzenes undergo during *trans-cis* photoisomerization drive these macromolecular phenomena. We additionally note that optimal response in terms of both SRG formation and birefringence is yet to be achieved using a dye concentration outside of the current study. Future work will focus on optimal architectures where a fraction of chromophores may be functionalized to maximize both mobility and mass motion in the same material, allowing for more effective AONP. Macromolecular post-functionalization using CuAAC 'click' chemistry of this class of azos provides a rapid and facile way to generate complex architectures, where the end groups may be given additional functionality.

Acknowledgements

AGH would like to acknowledge FQRNT for a B2 Doctoral Scholarship as well as a B3 Post-Doctoral Fellowship. TCC is funded through an NSERC-CREATE grant. The authors would like to thank Petr Fiuřasek for help in polymer characterization as well as the members of Zamboni Chemical Solutions: RZ, HZ, JC, MT for helpful discussions during synthesis.

Notes and references

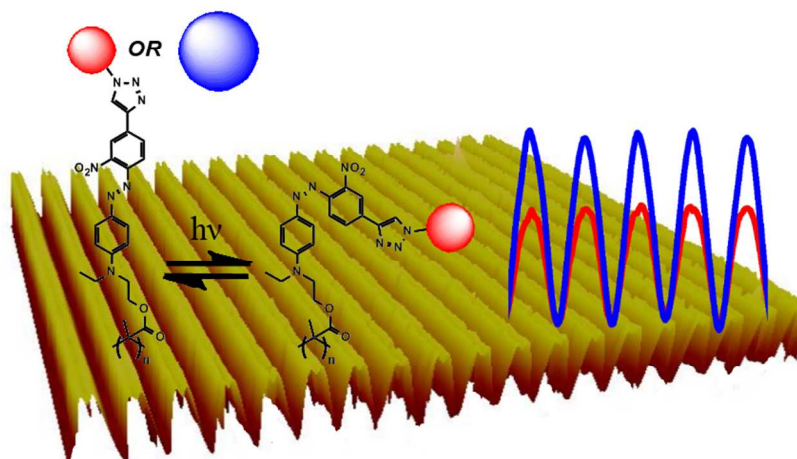
^a Department of Chemistry, McGill University, 801 Sherbrooke St. West, Montreal, QC, Canada, H3A 0B8.

^b Current Address: Department of Chemistry, Humboldt-Universität zu Berlin, Brook-Taylor-Str. 2, 12489 Berlin, Germany.

^c Aalto University, Optics and Photonics Group, Department of Applied Physics, P.O. BOX 13500, FI-00076 Aalto, Finland.

† Electronic Supplementary Information (ESI) available: Synthetic Details, ¹H, ¹³C, HRMS and GPC analysis of materials where appropriate and possible. Additional UV/vis as well as kinetic data from the optical testing of solutions and films. See DOI: 10.1039/b000000x/

- M. Poprawa-Smoluch, J. Baggerman, H. Zhang, H. P. A. Maas, L. De Cola, and A. M. Brouwer, *J. Phys. Chem. A*, 2006, **110**, 11926–11937.
- A. Natansohn and P. Rochon, *Chem. Rev.*, 2002, **102**, 4139–4175.
- Z. Mahimwalla, K. G. Yager, J. Mamiya, A. Shishido, A. Priimagi, and C. J. Barrett, *Polym. Bull.*, 2012, **69**, 967–1006.
- H. Koerner, T. J. White, N. V. Tabiryan, T. J. Bunning, and R. A. Vaia, *Mater. Today*, 2008, **11**, 34–42.
- K. G. Yager and C. J. Barrett, *Azobenzene Polymers for Photonic Applications*, John Wiley & Sons Ltd, Boca Raton, 2009.
- H. M. D. Bandara and S. C. Burdette, *Chem. Soc. Rev.*, 2012, **41**, 1809–1825.
- K. Uchida, S. Yamaguchi, H. Yamada, M. Akazawa, T. Katayama, Y. Ishibashi, and H. Miyasaka, *Chem. Commun.*, 2009, 4420–4422.
- O. M. Tanchak and C. J. Barrett, *Macromolecules*, 2005, **38**, 10566–10570.
- A. Priimagi and A. Shevchenko, *J. Polym. Sci., Part B Polym. Phys.*, 2014, **52**, 163–182.
- N. M. Ahmad, X. Lu, and C. J. Barrett, *J. Mater. Chem.*, 2010, **20**, 244–247.
- A. A. Beharry and G. A. Woolley, *Chem. Soc. Rev.*, 2011, **40**, 4422–4437.
- D. W. Jenkins, K. El-Tahlawy, A. El-Shafei, H. S. Freeman, and S. M. Hudson, *Color. Technol.*, 2006, **122**, 345–349.
- H. S. Freeman and S. A. McIntosh, *Text. Res. J.*, 1989, **59**, 343–349.
- M. G. Finn and V. V. Fokin, *Chem. Soc. Rev.*, 2010, **39**, 1231–1232.
- A. Goulet-Hanssens and C. J. Barrett, *Submitted*, 2014.
- H. A. Wegner, *Angew. Chem., Int. Ed.*, 2012, **51**, 4787–4788.
- O. Sadowski, A. Beharry, F. Zhang, and G. A. Woolley, *Angew. Chem., Int. Ed.*, 2009, **48**, 1484–1486.
- E. Merino, *Chem. Soc. Rev.*, 2011, **40**, 3835–3853.
- T. Caronna, F. Fontana, B. Marcandalli, and E. Selli, *Dye. Pigm.*, 2001, **49**, 127–133.
- Y. He, W. He, R. Wei, Z. Chen, and X. Wang, *Chem. Commun.*, 2012, **48**, 1036–1038.
- J. Vapaavuori, A. Priimagi, and M. Kaivola, *J. Mater. Chem.*, 2010, **20**, 5260–5264.
- D. Brown, A. Natansohn, and P. Rochon, *Macromolecules*, 1995, **28**, 6116–6123.
- K. G. Yager and C. J. Barrett, *J. Chem. Phys.*, 2004, **120**, 1089–1096.
- B. Hudson and B. Kohler, *Annu. Rev. Phys. Chem.*, 1974, **25**, 437–460.
- B. E. Kohler and I. D. W. Samuel, *J. Chem. Phys.*, 1995, **103**, 6248–6252.
- H. Nishioka, X. Liang, and H. Asanuma, *Chem.—Eur. J.*, 2010, **16**, 2054–2062.
- R. N. Jones, *Chem. Rev.*, 1947, **41**, 353–371.
- X. Wang, J. Kumar, S. K. Tripathy, L. Li, J.-I. Chen, and S. Marturunkakul, *Macromolecules*, 1997, **30**, 219–225.
- A. Priimagi, A. Shevchenko, M. Kaivola, F. J. Rodriguez, M. Kauranen, and P. Rochon, *Opt. Lett.*, 2010, **35**, 1813–1815.
- A. Priimagi, M. Kaivola, M. Virkki, F. J. Rodriguez, and M. Kauranen, *J. Nonlinear Opt. Phys. Mater.*, 2010, **19**, 57–73.
- U. Pietsch and P. Rochon, *J. Appl. Phys.*, 2003, **94**, 963.



TOC graphic
278x205mm (96 x 96 DPI)